Molecular Scale Speciation of First-Row Transition Elements Bound to Ligneous Material by Using X-ray Absorption Spectroscopy

Emmanuel Guillon,* Patricia Merdy, and Michel Aplincourt[a]

Abstract: To develop a solid scientific basis for maintaining soil quality and formulating effective remediation strategies, it is critical to determine how environmentally-important trace metals are sequestered in soils at the molecular scale. The speciation of Mn, Fe and Cu in soil organic matter has been determined by synchrotron-based techniques: extended X-ray absorption fine structure (EXAFS) and X-ray absorption near edge structure (XANES). We show the structural similarity between the surface complexes of Mn^{II}, Fe^{III} and Cu^{II}. These cations are bound to the surface through oxygen atoms. Each one presents a more or less tetragonal-distorted octahedral geometry. The use of X-ray absorption spectroscopy provides a relevant method for determining trace-metal speciation in both natural and contaminated environmental materials.

Keywords: adsorption · environmental chemistry · structure elucidation · surface chemistry · X-ray absorption spectroscopy

Introduction

The complexation of metal ions by soil organic matter (SOM) has become an important topic in environmental studies, because its understanding is closely related to the bioavailability, toxicity and mobility of metals in natural systems.[1–3] Especially, the knowledge of the chemical nature and stability of these complexes is a key point in the understanding of most reactions that occur in the soil environment, that is, ion exchange, precipitation – dissolution, redox properties, etc. It is now widely accepted that SOM, and notably lignin materials, plays a key role in the regulation of metal ions and other pollutants in the environment.[4–7] Lignin is a natural polymer that is biologically produced through random polymerisation processes, which makes its study complicated.[8] It is a cross-linked, phenolic polymer built from three basic phenyl propane monomers (*p*-hydroxycinnamyl, coniferyl and sinapyl alcohols), which are responsible for their chemical heterogeneity. While complexation of metal ions by humic substances is relatively well known, because widely studied, the implication of lignins in the holding-back of metals and the resulting transformation of organic matter are known only partially.

The determination of the geometrical structure of transition-metal surface complexes, especially lignin, is crucial for the understanding of their chemical behaviour, bioavailability and their migration in soils. To describe the surface complexation properties of metal ions in soils, on ligneous materials, one needs to obtain precise information on the interaction between these metal ions and lignin. The determination of the structure of organic surface complexes has been the subject of numerous studies in the last two decades. However, they were mainly focused on humic substances, which are organic soil material that is structurally comparable to lignocellulosic substrates. Although most of them were carried out by means of electron paramagnetic resonance (EPR),[9–12] special attention has recently been given to the use of X-ray absorption spectroscopy (XAS), by means of extended X-ray absorption fine structure (EXAFS) and X-ray absorption near edge structure (XANES) spectroscopies,[13–15] because it can provide precise information on the structure.

Thus, the aim of the present study is to use these two X-ray absorption techniques to characterise the transition-metal-surface systems. The material studied as the ligand for the metal ions is a lignocellulosic substrate (LS) extracted from wheat straw by acido – basic treatments. We report the results of a XANES and EXAFS examination of iron(III), manganese(II) and copper(II) surface complexes with LS, together with suitable model compounds. These three metal ions are of interest due to their abundance in soils.

[a] Dr. E. Guillon, Dr. P. Merdy, Prof. M. Aplincourt
GRECI (Groupe de Recherche En Chimie Inorganique)
Université de Reims Champagne-Ardenne
BP 1039, F-51687 Reims cedex 2 (France)
Fax : (+33) 3-26-91-32-43
E-mail: emmanuel.guillon@univ-reims.fr

Results and Discussion

Depending on the element, the pre-edge region of an X-ray absorption spectrum sometimes contains features of structural or electronic interest. Thus, features close to the

 DOI: 10.1002/chem.200304920

absorption edge can often be assigned to electronic transitions from 1s orbitals (*K*-edge) to higher bound states, the energies of which lie within the discrete part of the spectrum and give information about the valence state of the absorbing atom and its geometry. The edge itself defines the threshold ionisation energy, above which lies the continuum, with oscillations (XANES and EXAFS) superimposed on a smoothly varying background of photoelectron energy. These oscillations, called fine structure, reflect the electronic and geometric characteristics of the molecular environment of the chosen atom. In this paper, we use the discrete part of the spectra (pre-edge features) to establish the local geometry of the transition-metal atoms, and the EXAFS region to extract the bond lengths.

XANES studies and their first derivatives : It is usual to focus in XANES studies on energy shifts of absorption edges and particular features to learn about an element's oxidation state and chemical environment. Figure 1 shows the Cu *K*-edge XANES spectra of a) the Cu-LS compounds (including the model and reference compounds) and b) their first derivatives.

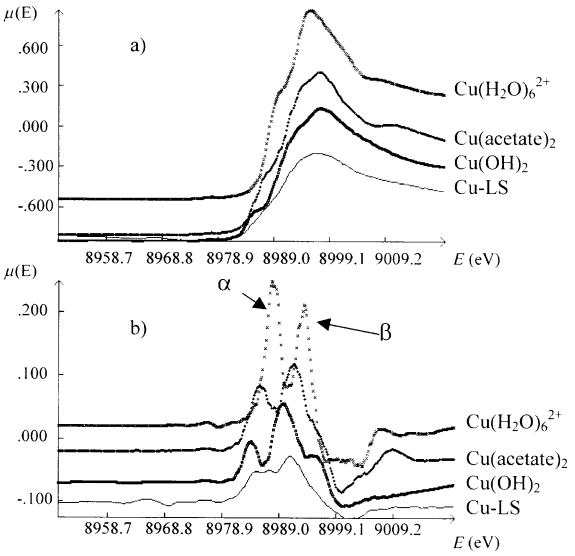

Figure 1. Cu *K*-edge XANES spectra of the sample and reference compounds (a), and their first derivatives (b).

A comparison of these XANES spectra reveals that they are almost identical, suggesting strong similarities in the geometry around the metal ion. Each model compound has more or less a tetragonally-distorted octahedral environment as the copper ion in Cu–LS complex, as it was shown by EPR spectroscopy experiments.[16] In XANES spectra of copper tetrahedral complexes, we can observe a weak $1s \rightarrow 3d$ transition pre-edge feature, and a shoulder on the low-energy side of the edge due to a $1s \rightarrow 4p$ transition. It is noteworthy that in XANES spectra of octahedral copper complexes, only a pre-edge bump due to $1s \rightarrow 3d$ transition exists.[17] Moreover, the intensity of this pre-edge feature is linked to the potential presence of a center of symmetry, and its intensity increases with the distortion from a symmetry due to the increase of p–d orbital mixing.[18]. Our Cu-LS XANES spectrum (Figure 1a) exhibits a very weak $1s \rightarrow 3d$ transition pre-edge feature centred around 8976 eV. A weak shoulder structure on the low-energy side of the edge was also observed, which reveals a tetragonal distortion.[19] However, the first derivative of the Cu–LS complex and model compound XANES spectra (Figure 1b) allows the precise quantification of splitting of the peaks α and β in each spectrum. The second main peak (β) represents the main absorption transition ($1s \rightarrow$ continuum). The energy gap between the α and β peaks is equal to 7 eV for $Cu(OH)_2$, 6 eV for $Cu(CH_3CO_2)_2$, 5.9 eV for Cu–LS and 5 eV for $CuSO_4 \cdot 5H_2O$. These values give an estimate of the destabilisation of the $4p_z$ metal orbital (z being the elongation axis), and are similar to those found for copper compounds in a square planar or tetragonally-distorted octahedral environments.[20–23] The average axial distance around the copper atom is equal to 2.63 Å for $Cu(OH)_2$, 2.42 Å for $Cu(CH_3CO_2)_2$ and 2.29 Å for $CuSO_4 \cdot 5H_2O$. The energy gap value of 5.9 eV for the Cu–LS surface complexes seems to indicate an axial Cu–O distance of approximately 2.40 Å, which is relatively high, in accordance with a strong tetragonal distortion. This value is close to those found by Palladino et al.[24] in an ATP complex, and by Alcacio et al.[23] and Xia et al.[21] in Cu^{II} bonding in humate complexes. These results are confirmed by the fact that the XANES region is sensitive to changes in the ligand environment and provides an independent measure for estimating how electron transitions and multiple scattering are influenced by adsorbed LS. The decrease in α peak intensity, compared to that of $[Cu(H_2O)_6]^{2+}$, shows that the Cu^{II} coordination environment depends on the ligand field. Actually, a decrease in the α peak intensity is expected, because the field of the water molecules undergoes ligand exchange with fields of different organic moieties (carboxylic or phenolic acids) in the equatorial plane. Moreover, the XANES region also contains information about electron transitions. It was found that the α peak intensity is influenced by the degree of axial distortion[25] and by the covalence of the equatorial ligands bonded to the Cu^{II} atom.[26] The source of the α electron transition has been attributed to a shakedown effect, whereby the final electron state is lower in energy than the direct $1s \rightarrow 4p$ transition.[26] The path to the final state involves a $1s \rightarrow 4p_z$ excitation combined with a ligand-to-metal charge transfer.[27] As demonstrated by the $[Cu(H_2O)_6]^{2+}$ spectrum (Figure 1b), water molecules coordinated in the equatorial plane produce a strong α peak intensity. When comparing the derivatives XANES spectra of Cu–LS to $[Cu(H_2O)_6]^{2+}$, the diminished α peak for the former suggests that LS is more sterically hindered due to its three-dimensional structure. Indeed, when Cu^{II} approached, it cannot bond in the equatorial plane with the same degree of angular overlap as water. Both two- and three-dimensional binding could be expected. However, such binding types are unlikely due to the relatively low site density equal to 0.8 nm^{-2}.[28] Such steric hindrance would affect the ability of the ligand to transfer charge to the metal when core electrons are removed in $1s \rightarrow 4p_z$ transitions. This also allowed us to conclude that copper(II) is held in an inner-sphere complex, as previously seen for other SOM copper

complexes.[29–32] The comparison between the XANES spectra of Cu–LS, $Cu(CH_3CO_2)_2$ and $Cu(OH)_2$ derivatives seems to indicate that binding sites for Cu^{2+} in LS preferentially involved carboxylic moieties, without excluding the phenolic groups. Indeed, the XANES spectrum of the Cu–LS derivative is the sum of those of $Cu(CH_3CO_2)_2$ and $Cu(OH)_2$, with a weight of approximately 50% and 50% respectively. Moreover, between the α and β Cu-LS peaks, a third peak appears, which seems to correspond to the α $[Cu(H_2O)_6]^{2+}$ peak. This is in accordance with the presence of two water molecules in axial position around copper ion (see EXAFS section).

Figure 2 shows the Fe *K*-edge XANES spectra of the Fe–LS compound and reference compounds. As in the Cu–LS system, the XANES spectra have a small pre-edge peak at

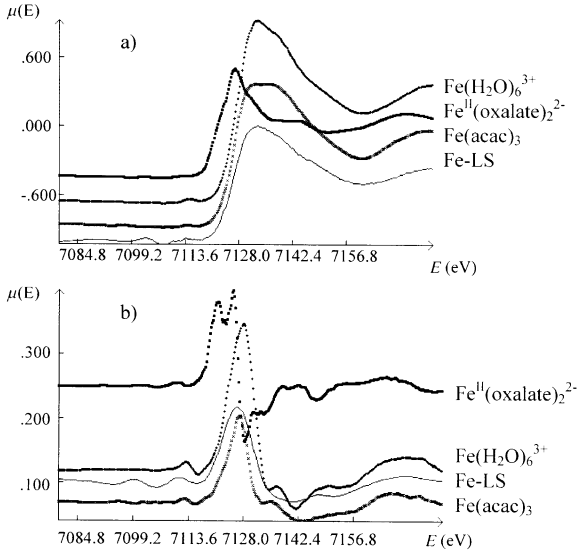

Figure 2. Fe *K*-edge XANES spectra of the sample and reference compounds (a), and their first derivatives (b).

~7113 eV assigned to a quadrupolar 1s → 3d transition.[33] The location and area of these peaks are very sensitive to the coordination symmetry.[33]. The amplitude of this pre-edge peak agrees with a six-coordinate complex with a relatively high symmetry, as previously shown by Que, Jr. and co-workers.[34, 35] Since oxido–reduction processes have been underlined at the LS surface,[7] an iron(II) reference compound was recorded. Its edge transition occurs at a smaller energy relative to the other compounds measured, especially Fe–LS; this indicates that iron is in the +III oxidation state at the LS surface. Unfortunately, in contrast to the Cu-LS system, it was not possible to conclude on which LS binding site iron(III) was sorbed. Indeed, XANES spectra of iron(III) compounds ($Fe(H_2O)_6^{3+}$, $Fe(acac)_3$ and Fe-LS) are too similar for us to form conclusions about the LS sites involved in the complexation.

The XANES spectrum of Mn-LS system at the Mn *K*-edge unequivocally shows that the oxidation state of the Mn atoms is +II. The X-ray absorption edge spectra of Mn-LS, $Mn(H_2O)_6^{2+}$, and $Mn(CH_3CO_2)_3^-$ are compared in Figure 3. While the edge features are significantly different, the

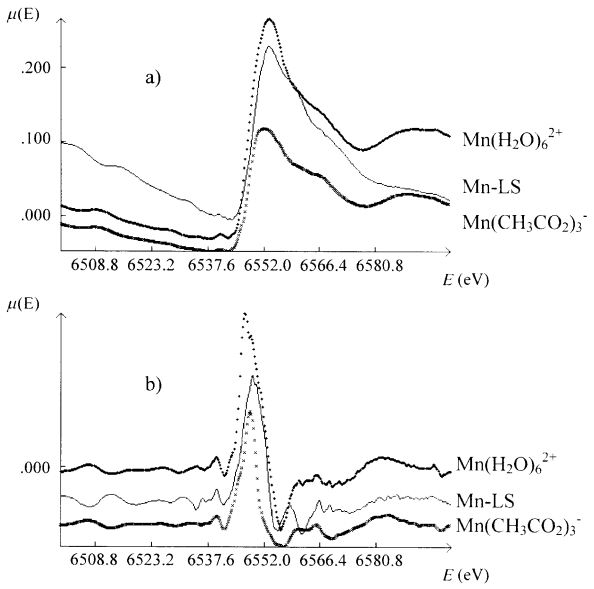

Figure 3. Mn *K*-edge XANES spectra of the sample and reference compounds (a), and their first derivatives (b).

absorption edge of Mn (assigned as the point of inflection in the absorption edge) is the same in each spectrum. The Mn^{II} edge spectrum has a pre-edge peak at ~10 eV below the point of inflection. The peak arises from the 1s → 3d transition, which is forbidden by the dipole selection rule, but occurs due to quadrupole and symmetry-breaking effects. As for the iron compounds, the area under the peak is sensitive to the coordination geometry and symmetry of the complex, being smallest for regular octahedral complexes.[34, 35]. In Figure 3, the 1s → 3d peak for $Mn(H_2O)_6^{2+}$ and $Mn(CH_3CO_2)_3^-$ is barely observable; this is consistent with a regular octahedral geometry. The 1s → 3d peak for the Mn–LS complex is slightly more intense, suggesting that the Mn atoms are six-coordinate, but that the averaged symmetry of the coordination shells is lower than in $Mn(H_2O)_6^{2+}$. Lower symmetry could be associated with larger differences among the Mn–LS bond lengths.[18].

EXAFS analysis: Table 1 summarises the number of nearest-neighbour atoms and their distances from the respective metal centres. The relatively large Debye–Waller factors in the first shell Fe–O and Mn–O distances are ascribed to the local geometric distortion of Fe^{III} and Mn^{II}. Moreover, for Mn^{II}, a relatively weak metal binding could also be considered.[13]

Cu-EXAFS: The k^3-weighted EXAFS spectrum with the theoretical simulation for Cu–LS system is shown in Figure 4a. The Fourier transformed EXAFS function (Figure 4b) shows a predominant first coordination shell peak. No high *Z* backscatterers are evident beyond this first shell, which indicates that no metal–metal bond, co-precipitation or polymerisation effects occur. The weak scattering contribution from low *Z* elements beyond the first shell to the EXAFS, seen as minor Fourier peaks, prevents a more detailed analysis. Within the framework of the single scattering approach, the Cu–LS EXAFS signal fits well (see Table 1),

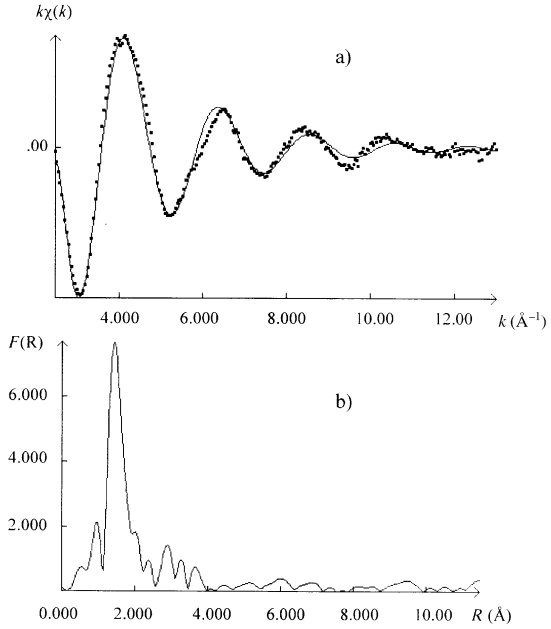

Figure 4. a) Experimental (· ··) and fitted (——) EXAFS *k* space spectra of Cu-LS system. b) Fourier transform of the EXAFS signal ($k^3\chi(k)$) at the copper *K*-edge.

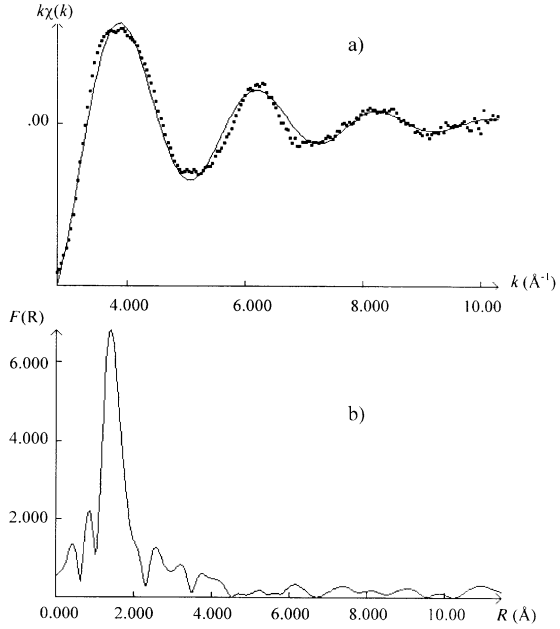

Figure 5. a) Experimental (· ··) and fitted (——) EXAFS *k* space spectra of Fe-LS system. b) Fourier transform of the EXAFS signal ($k^3\chi(k)$) at the iron *K*-edge.

Table 1. EXAFS results at the metal *K* edge for the metal–LS systems.

	Absorber–scatterer	*N*	*R* [Å][a]	σ [Å^2]	ΔE [eV]
Cu–LS	Cu–O	3.97	1.93	0.002	1.12
	Cu–O	1.84	2.41	0.012	10.21
Fe–LS	Fe–O	5.73	1.99	0.005	−3.77
Mn–LS	Mn–O	6.32	2.17	0.006	−0.78

[a] The errors in the distances are in the range of ±0.02 Å.

and indicates that Cu^{II} ions are surrounded by four oxygen atoms, and two other oxygen atoms with average Cu–O bond lengths of 1.93 and 2.41 Å, respectively, with a least-squares fitting parameter of 2%. The goodness of the fit can be seen in Figure 4a. These data are consistent with those obtained from XANES spectrum, that is, a strong tetragonal-distorted octahedral coordination around copper(II) in LS. These results are close to those obtained in other similar natural organic substrate.[13, 23, 29, 36, 37]

Fe-EXAFS: The unfiltered and Fourier transformed EXAFS region spectra of Fe-LS system are displayed in Figure 5 (a and b, respectively). Experimental Fe *K*-edge EXAFS interference function shown in Figure 5a has an oscillation frequency up to a photoelectron momentum value of ~ 9 Å^{-1}; this suggests that only the first nearest Fe–O shell is resolved in our spectrum. This conjecture is confirmed from the observation of the corresponding Fourier transform spectrum shown in Figure 5b. Specifically, in this phase shift uncorrected radial distribution function a next nearest neighbour shell is not clearly observed. Its magnitude is, unfortunately, too small to deliver any meaningful information. The results from the best fit are shown in Table 1. The EXAFS region of the Fe–LS complex refined well for a surface complex containing six oxygen scatterers at the distance of 1.99 Å from the metal centre (fitting parameter of 1.4%). The coordination number found by XAS is in accordance with the octahedral geometry obtained by EPR spectroscopy.[7] The average Fe–O distance of 1.99 Å is very close to that obtained for iron(III) bound to humic acids.[13]

Mn-EXAFS: The EXAFS spectrum of the Mn–LS system was interpreted by using a single shell model, in agreement with the single major peak in the Fourier transform (Figure 6). An adequate fit (fitting parameter of 1.1%) was obtained by a

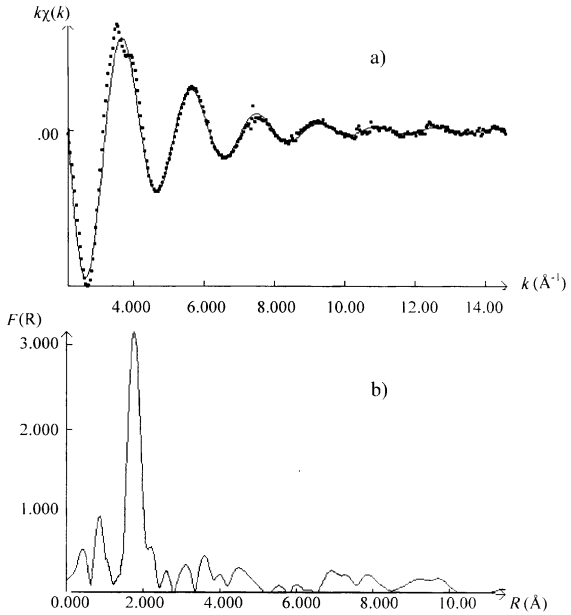

Figure 6. a) Experimental (· ··) and fitted (——) EXAFS *k* space spectra of Mn-LS system. b) Fourier transform of the EXAFS signal ($k^3\chi(k)$) at the manganese *K*-edge.

single shell of six oxygen atoms with an average Mn–O distance of 2.17 Å (Table 1). The Debye–Waller factor (σ = 0.006 Å^2) was relatively high in comparison with the values normally found for the first shell backscatterers. This is consistent with static disorder (i.e., the average of several similar Mn–ligand distances), and it is in accordance with XANES spectrum. Thus the EXAFS, XANES, and EPR[7] results consistently indicate a slightly distorted octahedral coordination around manganese.

Conclusion

XAS provides reliable information for metal–SOM surface complexes. This study is, to our knowledge, the first one that describes, at the atomic scale, structural information on natural abundant metallic cations sorbed onto a lignocellulosic substrate, which is the main soil component with humic substances. The series examined in the present study show that metallic cations are sorbed onto LS by oxygen atoms. The results are consistent with inner-sphere surface Cu^{II} and Fe^{III} complexes, and outer-sphere complexes for Mn^{II}, in accordance with EPR studies.[7, 16] Copper(II) is surrounded by four oxygen atoms at 1.93 Å and two other ones at 2.41 Å, which corresponds to a tetragonal-distorted octahedral geometry. On the other hand, iron(III) and manganese(II) are surrounded by six oxygen atoms at 1.99 and 2.17 Å, respectively. These results may be useful in developing sound remediation strategies for soils contaminated with first row transition metals.

Experimental Section

Potassium nitrate KNO_3, manganese nitrate $Mn(NO_3)_2 \cdot 4H_2O$, ferric nitrate $Fe(NO_3)_3 \cdot 9H_2O$, and copper nitrate $Cu(NO_3)_2 \cdot 3H_2O$ were purchased from Fluka. All chemicals from commercial sources were of the highest available purity and have been used without further purification.

Sample preparation : The lignocellulosic substrate (LS) was extracted from wheat straw. The natural straw was subjected to two successive treatments : 1) an acidic hydrolysis (H_2SO_4 10% wt/wt of dry matter) to remove starch, proteins, and sugars; and 2) an alkali treatment (NaOH 0.02 mol L^{-1}, T_{amb}, 1 day stirring) to dissolve the low molecular-weight lignin compounds. Such treatments lead to an insoluble substrate, for a pH ranging from 2 to 10, suitable for the sorption of metallic cations. The solid (2 g L^{-1}) was then stirred with a solution of HNO_3 (0.04 mol L^{-1}) over 3 h in order to protonate all acid sites, and washed with de-ionised water until the pH of the filtrate reached a constant value. The protonation of all acid sites has been checked by potentiometric titrations.[30] The powder obtained was dried under vacuum and ground to pass a 100 μm sieve.

IR and ^{13}C-CP/MAS NMR spectroscopy and XPS lead us to identify carboxylic and phenolic moieties as the main functional groups.[28] The content of acidic surface sites was estimated by using ion exchange reactions and potentiometric titrations in aqueous and non-aqueous media. We determined a concentration of 0.09×10^{-3} and 0.48×10^{-3} mol g^{-1} for carboxylic and phenolic moieties, respectively.[30]

Manganese–, iron–, and copper–LS surface complexes were prepared by dispersing LS (1 g) in a solution (500 mL) that contained the metal nitrate (10^{-3} mol L^{-1}) and the supporting electrolyte KNO_3 (0.1 mol L^{-1}). The pH of the suspensions was controlled regularly with a pH-meter (Metrohm 655) equipped with a glass electrode paired with an internal standard Ag/AgCl/KCl reference and adjusted by adding HNO_3 (0.1 mol L^{-1}) and NaOH (0.1 mol L^{-1}) to its equilibrium value. The pH values have been chosen to ensure a good sorption capacity, and were equal to 8.5, 3.3, and 5.75 for Mn^{II}, Fe^{III}, and Cu^{II} ions, respectively. The suspensions were stirred with an automatic shaker at 20 °C for 12 hours to reach sorption equilibrium. They were then filtered through a 0.2 μm pore cellulosic acetate membrane and the solids were dried under vacuum. Free metal ions in the filtrate were analysed by using a Varian Liberty ICP/AES spectrometer. The amount of metal adsorbed was calculated from the initial concentration.

X-ray absorption data collection and processing : The XANES (X-ray absorption near edge structure) and EXAFS (extended X-ray absorption fine structure) data were collected at LURE (Laboratoire d'Utilisation du Rayonnement Electromagnétique, Paris-Sud University) on the XAS 4 beam line of the storage ring DCI (positron energy 1.85 GeV; mean current 300 mA). The spectra were recorded at transition-metal *K*-edge using the channel-cut monochromator (Si(111) for EXAFS and Si(311) for XANES), which was detuned to 30% and 10% of the maximum intensity for Mn and Fe, respectively, to remove the higher order harmonics. The energy was calibrated by using Mn, Fe and Cu metallic foils and fixed at 6556.6, 7131.3 and 8979 eV, respectively, for the first inflection point of the metallic foil spectra. The measurements were performed at room temperature in the transmission mode with two air-filled ionisation chambers.

The XANES spectra were recorded step-by-step, every 0.3 eV with a 2 s accumulation time per point. The spectra of the 5 μm metallic foils were recorded just before the unknown XANES spectra to check the energy calibration, thus ensuring an energy accuracy of 0.25 eV. The EXAFS spectra were recorded over 1000 eV, with 2 eV steps, from 6400 to 7400, from 7000 to 8000 and from 8900 to 9900 eV for manganese, iron and copper compounds, respectively. Data analysis was performed by means of the "EXAFS pour le Mac" package.[38] The $\chi(k)$ functions were extracted from the data with a linear pre-edge background, a combination of polynomials and spline atomic-absorption background, and normalised by using the Lengeler–Eisenberg method.[39] The energy threshold, E_0, was taken at the middle of the absorption edge. E_0 was corrected for each spectrum in the fitting procedure. The k^3-weighted $\chi(k)$ function was Fourier transformed from k = 2–14 or 2–12 Å^{-1}, by means of a Kaiser–Bessel window with a smoothness parameter equal to 3 (k is the photoelectron wave number). In this work, all Fourier transforms were calculated and presented without phase correction. The peaks corresponding to the first- or two first-coordination shells were then isolated and back-Fourier transformed into k space to determine the mean coordination number (N), the bond length (R) and the Debye–Waller factor (σ) by a fitting procedure realised in the framework of single scattering. Before this, we used the FEFF7 code[40] to check if the multiple scattering of our reference compounds of known crystallographic structure[41, 42] is negligible in the 0–2.8 Å range (see text) and to calculate the ab initio amplitude and phase functions, $|f_i(k,R_i)|$ and $|\phi_i(k,R_i)|$, respectively.

Acknowledgement

We would like to thank Dr. S. Belin (Université Paris-sud, LURE, France) for her help in XAS data recording and for helpful discussions.

[1] W. Stumm, J. J. Morgan, *Aquatic Chemistry*, 2nd ed., Wiley, New-York, **1996**, Chapter 6.
[2] " Soil Processes and the Behaviour of Metals" B. J. Alloway, in *Heavy Metals in Soils* (Ed.: B. J. Alloway), Blackie, London, **1990**, pp. 7–28.
[3] P. Duchaufour, *Pédologie 1. Pédogénèse et Classification*, Masson, Paris, **1983**.
[4] J. C. Echeverria, M. T. Morera, C. Mazkiaran, J. J. Garrido, *Environ. Pollut.* **1998**, *101*, 275.
[5] S. E. Bailey, T. J. Olin, R. M. Bricka, D. D. Adrian, *Water Res.* **1999**, *33*, 2469.
[6] A. Kokorevics, J. Gravitis, E. Chirkova, O. Bikovens, N. Druz, *Cell. Chem. Technol.* **1999**, *33*, 251.
[7] P. Merdy, E. Guillon, M. Aplincourt, *New J. Chem.* **2002**, *26*, 1638.
[8] E. Ammälahti, G. Brunow, M. Bordet, D. Robert, I. Kilpeläinen, *J. Agric. Food Chem.* **1998**, *46*, 5113.
[9] N. Senesi, S. M. Griffith, M. Schnitzer, *Geochim. Cosmochim. Acta* **1977**, *41*, 969.

[10] N. Senesi, *Anal. Chim. Acta* **1990**, *232*, 51.
[11] S. Al Asheh, G. Lamarche, Z. Duvnjak, *Water Qual. Res. J. Can.* **1998**, *33*, 167.
[12] T. Oniki, *J. Wood Sci.* **1998**, *44*, 314.
[13] G. Davies, A. Fataftah, A. Cherkasskiy, E. A. Ghabbour, A. Radwan, S. A. Jansen, S. Kolla, M. D. Paciolla, L. T. Sein Jr., W. Buermann, M. Balasubramanian, J. Budnick, B. Xing, *J. Chem. Soc. Dalton Trans.* **1997**, 4047.
[14] K. Xia, W. Bleam, P. A. Helmke, *Geochim. Cosmochim. Acta* **1997**, *61*, 2211.
[15] G. Sarret, J. Vangronsveld, A. Manceau, M. Musso, J. D'Haen, J. J. Menthonnex, J. L. Hazemann, *Environ. Sci. Technol.* **2001**, *35*, 2854, and references therein.
[16] P. Merdy, E. Guillon, M. Aplincourt, J. Dumonceau, H. Vezin, *J. Colloid Interface Sci.* **2002**, *245*, 24.
[17] A. Bianconi, M. Dell'Ariccia, P. J. Durham, J. B. Pendry, *Phys. Rev. B* **1982**, *26*, 6502.
[18] J. E. Hahn, R. A. Scott, K. O. Hodgson, S. Doniach, S. Desjardins, E. I. Solomon, *Chem. Phys. Lett.* **1982**, *88*, 595.
[19] N. Kosugi, T. Yokoyama, K. Asakuna, H. Kuroda, H., *Chem. Phys.* **1984**, *91*, 249.
[20] C. Surville-Barland, R. Ruiz, A. Aukauloo, Y. Journaux, I. Castro, B. Cervera, M. Julve, F. Llord, F. Sapina, *Inorg. Chim. Acta* **1998**, *278*, 159.
[21] K. Xia, A. Mehadi, R. W. Taylor, W. F. Bleam, *J. Colloid Interface Sci*. **1997**, *185*, 252.
[22] D. C. Bull, P. W. Harland, G. J. Foran, *J. Wood Sci.* **2000**, *46*, 248.
[23] T. E. Alcacio, D. Hesterberg, J. W. Chou, J. D. Martin, S. Beauchemin, D. E. Sayers, *Geochim. Cosmochim. Acta* **2001**, *65*, 1355.
[24] L. Palladino, S. Della Longa, A. Keale, M. Belli, A. Scafati, G. Onori, A. Santucci, *J. Chem. Phys.* **1993**, *98*, 2720.
[25] J. Garcia, M. Benfatto, C. R. Natoli, A. Bianconi, A. Fontaine, H. Tolentino, *Chem. Phys.* **1989**, *132*, 295.
[26] L. S. Kau, D. J. Spira-Solomon, J. E. Penner-Hahn, K. O. Hodgson, E. I. Solomon, *J. Am. Chem. Soc.* **1987**, 6433.
[27] R. A. Blair, W. A. Goddard, *Phys. Rev. B* **1980**, *22*, 2767.
[28] P. Merdy, E. Guillon, J. Dumonceau, M. Aplincourt, *Anal. Chim. Acta* **2002**, *459*, 133.
[29] P. Merdy, E. Guillon, J. Dumonceau, M. Aplincourt, *Environ. Sci. Technol.* **2002**, *36*, 1728.
[30] E. Guillon, P. Merdy, M. Aplincourt, J. Dumonceau, H. Vezin, *J. Colloid Interface Sci*. **2001**, *239*, 39.
[31] N. Senesi, *Anal. Chim. Acta* **1990**, *232*, 51.
[32] M. McBride, *Soil Sci.* **1978**, *126*, 200.
[33] J. Zhao, F. E. Huggins, Z. Feng, F. Lu, N. Shah, G. P. Huffmann, *J. Catal.* **1993**, *143*, 499.
[34] A. L. Roe, D. J. Schneider, R. J. Mayer, J. W. Pyrz, J. Widom, L. Que, Jr., *J. Am. Chem. Soc.* **1984**, *106*, 1676.
[35] C. R. Randall, L. Shu, Y. Chiou, K. S. Hagen, M. Ito, N. Kitajima, R. J. Lachicotte, Y. Zang, L. Que, Jr., *Inorg. Chem.* **1995**, *34*, 1036.
[36] L. Dupont, E. Guillon, J. Bouanda, J. Dumonceau, M. Aplincourt, *Environ. Sci. Technol.* **2002**, *36*, 5062.
[37] K. Xia, A. Mehadi, R. W. Taylor, W. F. Bleam, *J. Colloid Interface Sci*. **1997**, *185*, 252.
[38] A. Michalowicz, EXAFS pour le Mac, Logiciel pour la Chimie, Société Française de Chimie, Paris **1991**, p. 102.
[39] B. Lengeler, P. Eisenberg, *Phys. Rev. B* **1980**, *21*, 4507.
[40] S. I. Zabinsky, J. J. Rehr, A. Ankudinov, R. C. Albers, M. J. Eller, *Phys. Rev. B.* **1995**, *52*, 2995.
[41] M. L. Hu, Z. M. Jin, Q. Miao; L. P. Fang, *Z. Kristallogr.* **2001**, *216*, 597.
[42] J. N. Van Niekerk, K. R. L. Schoening, *Acta Crystallogr.* **1953**, *6*, 227.

Received: March 6, 2003 [F4920]